

Stability studies on a Spherical Inertial Electrostatic Confinement

H. J. Kim*

Nuclear, Plasma, and Radiological Engineering
University of Illinois at Urbana-Champaign, Urbana, Illinois 61801

Fermi National Accelerator Laboratory
July 11, 2006

*hjkim2@uiuc.edu

Outline

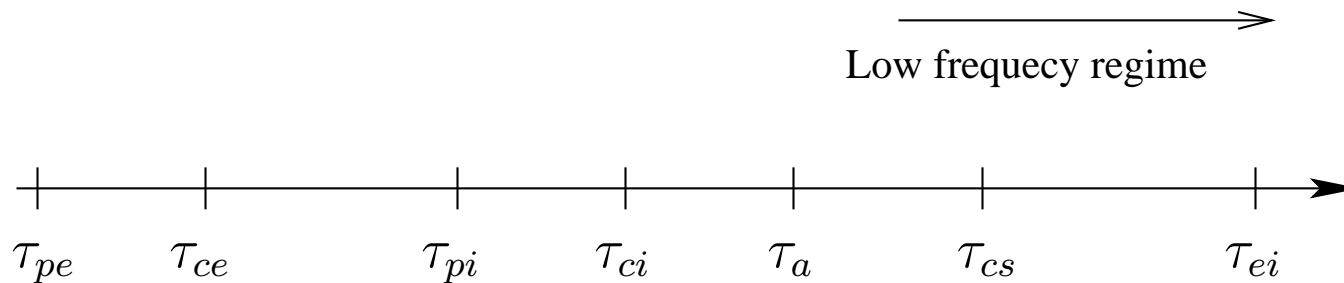
- Fully Implicit Particle-in-Cell
 - ▷ Motivation
 - ▷ FIPIC Algorithm
 - ▷ Numerical examples
- Stability Study on Spherical Inertial Electrostatic Confinement
 - ▷ Motivation
 - ▷ Nonlocal theory
 - ▷ δf Particle-in-Cell method
 - ▷ Results
- Summary

Fully Implicit Particle-in-Cell Algorithm

Motivation

□ Explicit Method:

- ▷ It is simple and straightforward to implement, BUT is **inappropriate for multiple time scale problems** since they must resolve the fastest time scale supported by the model ($\omega_{pe}^{-1} / \omega_{pi}^{-1} = \sqrt{m_e / m_i}$, $\omega_{pe} \Delta t < 1$).
- ▷ **Numerical stability constraint on the grid spacing**, $\Delta x < \lambda_{De}$, to avoid the finite-grid instability.



Motivation

□ Semi-Implicit Method:

- ▷ Decouple Poisson equation from the equation of motion, but still implicit. → no constraints as for explicit method (typically, $\Delta t_{\text{implicit}}/\Delta t_{\text{explicit}} \sim 10^2$, $\Delta x_{\text{implicit}}/\Delta x_{\text{explicit}} \sim 10^2$).
- ▷ Particle and field quantities are inconsistent at the each time step. → possibly poor energy conservation.

$$\mathbf{x}_i^{n+1} = \mathbf{x}_i^n + \mathbf{v}_i^{n+1/2} \Delta t,$$

$$\mathbf{v}_i^{n+1} = \mathbf{v}_i^n + \Delta t \frac{q}{m} \mathbf{E}^{n+\theta} \left(\mathbf{x}_i^{n+1/2} \right),$$

$$\nabla \cdot \mathbf{E}^{n+\theta} = 4\pi \rho^{n+\theta}$$

↓

$$\nabla \cdot \left[\left(1 + \frac{\theta (\Delta t)^2}{2} \sum_{\sigma} \frac{q_{\sigma}}{m_{\sigma}} \rho_{\sigma}^n \right) \mathbf{E}^{n+\theta} \right] = 4\pi \left(\rho^n - \theta \Delta t \nabla \cdot \mathbf{j}^n \right)$$

Motivation

□ Explicit Method:

- ▷ It is simple and straightforward to implement, BUT is **inappropriate for multiple time scale problems** since they must resolve the fastest time scale supported by the model ($\omega_{pe}^{-1} / \omega_{pi}^{-1} = \sqrt{m_e / m_i}$, $\omega_{pe} \Delta t < 1$).
- ▷ **Numerical stability constraint on the grid spacing**, $\Delta x < \lambda_{De}$, to avoid the finite-grid instability.

□ Semi-Implicit Method:

- ▷ Decouple Poisson equation from the equation of motion, but still implicit. → no constraints as for explicit method (typically, $\Delta t_{\text{implicit}} / \Delta t_{\text{explicit}} \sim 10^2$, $\Delta x_{\text{implicit}} / \Delta x_{\text{explicit}} \sim 10^2$).
- ▷ **Particle and field quantities are inconsistent** at the each time step. → **possibly poor energy conservation**.

□ Fully-Implicit Method:

- ▷ **Achieve consistency between particle and field quantities** at the each time step. → **improve energy conservation**.
- ▷ To do this, both particle and Poisson equations are packed inside the nonlinear solver such as Newton-Krylov solver.

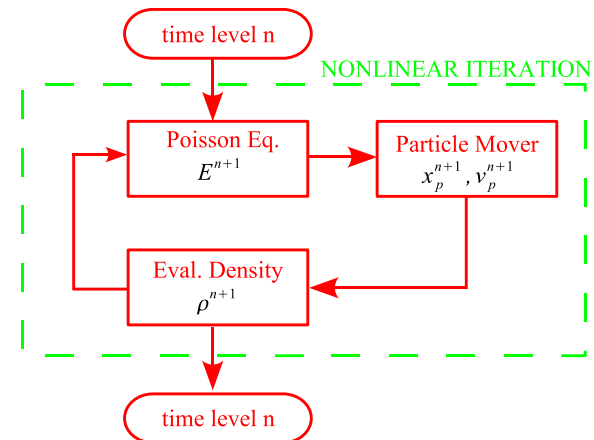
Fully Implicit Particle-in-Cell(FIPIC) Method

- Electrostatic case is presented here. Extension to electromagnetic problem is straightforward with some consideration.
- The FIPIC method uses **the nonlinear function (of Poisson equation) as a measure of convergence of the coupled system.**
- The coupled system is **packed inside the nonlinear solver** such as Newton-Krylov.
- The convergence of the nonlinear function F guarantees that one get the **self-consistent solutions of particles' equation of motion and Poisson equation**, because the particle and the field equations are evaluated iteratively inside a nonlinear solver.
- The **nonlinear residual** is given by

$$F(\psi^{n+\theta,k}) = \nabla^2 \psi^{n+\theta,k} + \rho(\psi^{n+\theta,k})$$

$$\vec{\xi}_i^{n+1} = \vec{\xi}_i^n + \Delta\tau \vec{v}_i^{n+1/2}$$

$$\vec{v}_i^{n+1} = \vec{v}_i^n + \frac{q}{m} \vec{E}^{n+1/2}(\vec{\xi}_i^{n+1/2})$$



where n the time step, k the k th Newton iteration, and θ the time decentering.

- **Jacobian-free Newton-Krylov** technique is employed for the nonlinear solver.

Jacobian-free Newton-Krylov (JFNK) Methods

- JFNK is a way to solve efficiently the nonlinear system $\vec{F} = 0$ using Newton and Krylov methods.
- Newton's method is a generalized iterative process to find accurate roots of a nonlinear equation, $\vec{F}(\vec{u}) = 0$.

$$\mathbf{J}^k \delta \vec{u}^k = -\vec{F}(\vec{u}^k), \quad \text{with} \quad \vec{u}^{k+1} = \vec{u}^k + \delta \vec{u}^k, \quad (1)$$

where \mathbf{J}^k is the Jacobian matrix of which the element (i, j) is $J_{i,j}^k = \frac{\partial F_i}{\partial u_j}$.

- The solution of Eq. (1) is constructed by spanning the Krylov subspace in the following form

$$\delta \vec{u}_l^k = \sum_{i=0}^{l-1} a_i \mathbf{J}^i \vec{r}_0, \quad (2)$$

where l is the linear iteration number, and \vec{r}_0 is the initial linear residual.

- Jacobian-free implementation is done by

$$\mathbf{J}^k \vec{r} = \frac{\vec{F}(\vec{u}^k + \epsilon \vec{r}) - \vec{F}(\vec{u}^k)}{\epsilon} \quad (3)$$

JFNK Methods (continued)

- For efficiency, an **inexact Newton** method is usually employed

$$\frac{\left\| \mathbf{J}^k \delta \vec{u}^k + \vec{F}(\vec{u}^k) \right\|}{\left\| \vec{F}(\vec{u}^k) \right\|} < \eta_k. \quad (4)$$

Here, η_k is a forcing term whose selection determines the order of convergence of the inexact Newton method.

- In Jacobian-free application, **right preconditioning** is often employed so that one solves

$$\mathbf{J}^k \mathbf{P}^{-1} (\mathbf{P} \delta \vec{u}^k) = -\vec{F}(\vec{u}^k), \quad (5)$$

where \mathbf{P} is the preconditioner.

- The **matrix-vector product for right preconditioning** is

$$\mathbf{J}^k \mathbf{P}^{-1} \vec{r} = \frac{\vec{F}(\vec{u}^k + \epsilon \mathbf{P}^{-1} \vec{r}) - \vec{F}(\vec{u}^k)}{\epsilon}, \quad (6)$$

and the preconditioned linear system, Eq. (5), is solved in two steps: **solve** $(\mathbf{J}^k \mathbf{P}^{-1}) \vec{w}^k = -\vec{F}(\vec{u}^k)$ for \vec{w}^k , and then solve $\delta \vec{u}^k = \mathbf{P}^{-1} \vec{w}^k$.

Preconditioner of Electrostatic System

- Efficient preconditioner **reduces the number of Krylov iterations considerably**.
- **Differential form of preconditioner** is derived from **approximating the Jacobian** ($J^k = \nabla^2 + \partial\rho/\partial\psi^k$) for the nonlinear Poisson equation.
- $\partial\rho/\partial\psi^k$ can be rewritten by the shape function and the chain rule:

$$\left. \frac{\partial\rho}{\partial\psi} \right|_{\psi^k} = \frac{\partial}{\partial\psi} \sum_{\sigma} \sum_{j \in \sigma} q_j S(\vec{\xi} - \vec{\xi}_j) \Big|_{\psi^k} = \sum_{\sigma} \sum_{j \in \sigma} q_j \left. \frac{\partial S}{\partial \vec{\xi}_j} \right|_{\psi^k} \cdot \left. \frac{\partial \vec{\xi}_j}{\partial \psi} \right|_{\psi^k}.$$

- Antisymmetry of shape function and temporal discretization of equation of motion give

$$\left. \frac{\partial\rho}{\partial\psi} \right|_{\psi^k} = -\frac{\partial}{\partial \vec{\xi}} \cdot \sum_{\sigma} \sum_{j \in \sigma} q_j S(\vec{\xi} - \vec{\xi}_j^k) \left. \frac{\partial \vec{\xi}_j}{\partial \psi} \right|_{\psi^k} = -(\theta\Delta t)^2 \frac{\partial}{\partial \vec{\xi}} \cdot \frac{\partial}{\partial \psi} \left[\sum_{\sigma} \frac{q_{\sigma}}{m_{\sigma}} \rho_{\sigma}^k \vec{E} \right]_{\psi^k}.$$

- Further, we obtain

$$\left. \frac{\partial\rho}{\partial\psi} \right|_{\psi^k} = (\theta\Delta t)^2 \frac{\partial}{\partial \vec{\xi}} \cdot \left[\sum_{\sigma} \frac{q_{\sigma}}{m_{\sigma}} \rho_{\sigma}^k \frac{\partial}{\partial \vec{\xi}} \right].$$

- Finally, **preconditioner for electrostatic system** is given by

$$P = \nabla_{\vec{\xi}} \cdot \left[\left(1 + (\theta\Delta t)^2 \sum_{\sigma} \frac{q_{\sigma}}{m_{\sigma}} \rho_{\sigma} \right) \nabla_{\vec{\xi}} \right]. \quad (7)$$

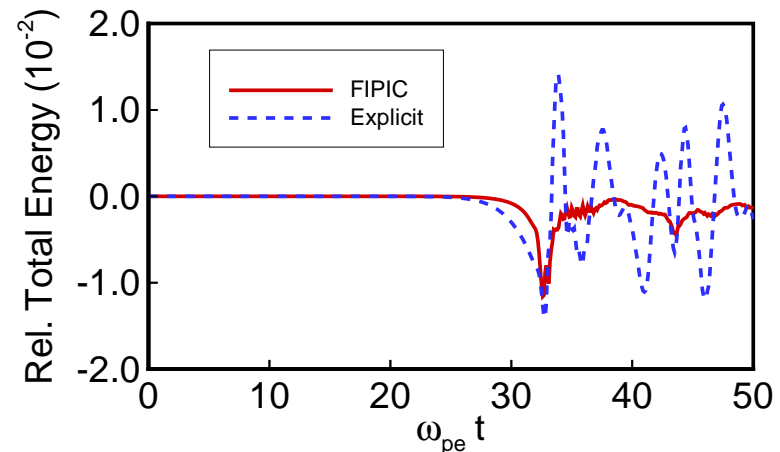
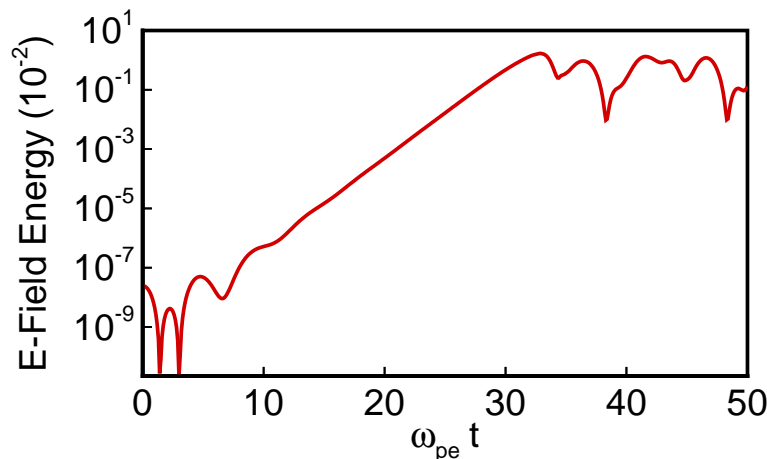
Fully Implicit Particle-in-Cell Algorithm

- 1: \vec{x}_j^n and u_j^n are given
- 2: $\vec{r}_0 \leftarrow \left\| \vec{F} \left(\vec{\psi}^{n,k=0} \right) \right\|$
- 3: **while** $\left\| \vec{F} \left(\vec{\psi}^{n+\theta,k+1} \right) \right\| > \tau_{rel} \vec{r}_0 + \tau_{abs}$ **do**
- 4: **while** $\left\| \mathbf{J}^k \delta \vec{\psi}^{n+\theta,k} + \vec{F} \left(\vec{\psi}^{n+\theta,k} \right) \right\| < s_k \left\| \vec{F} \left(\vec{\psi}^{n+\theta,k} \right) \right\|$ **do**
- 5: solve nonlinear Newton's equations:
- 6: $\vec{u}_j^{n+1,k} \leftarrow \vec{u}_j^{n,k} + \Delta t \frac{q}{m} \vec{E}_j^{n+1/2,k}$
- 7: $\vec{\xi}_j^{n+1,k} \leftarrow \vec{\xi}_j^{n,k} + \Delta t \vec{u}_j^{n+1/2,k}$
- 8: $\rho^{n+\theta,k} \leftarrow \sum_{\sigma} \sum_{j \in \sigma} q_j S \left(\vec{\xi} - \vec{\xi}_j^{n+\theta,k} \right)$
- 9: $\vec{F}^{n+\theta,k} \leftarrow \nabla^2 \vec{\psi}^{n+\theta,k} - \rho \left(\vec{\psi}^{n+\theta,k} \right)$
- 10: minimize $\left\| \mathbf{J}^k \delta \vec{\psi}^{n+\theta,k} + \vec{F} \left(\vec{\psi}^{n+\theta,k} \right) \right\|$ to obtain $\delta \vec{\psi}^{n+\theta,k}$
- 11: **end while**
- 12: $\vec{\psi}^{n+\theta,k+1} \leftarrow \vec{\psi}^{n+\theta,k} + \delta \vec{\psi}^{n+\theta,k}$
- 13: evaluate $\vec{F} \left(\vec{\psi}^{n+\theta,k+1} \right)$
- 14: **end while**

Numerical Test(1): Electron Two Stream Instability

- **Equilibrium: uniform density** ($n_i = n_e = n_0$), $\vec{E} = 0$, and unmagnetized.
- Immobile ions and **two cold electron beams** with $v_0 = \pm \frac{\sqrt{3}}{2\sqrt{2}}\omega_{pe}/k$.
- 1D domain of 32 grids, 10^5 simulation particles, and $\omega_{pe}\Delta t = 0.1$ **time step**.
- Perturb. electron density: $\delta n/n_e = \epsilon \cos(k_0\xi)$ with $k_0 = 2\pi$ and $\epsilon = 10^{-3}$.
- Linear growth rate $\gamma_{\text{theoretical}} = 0.354$, $\gamma_{\text{simulation}} = 0.341$.

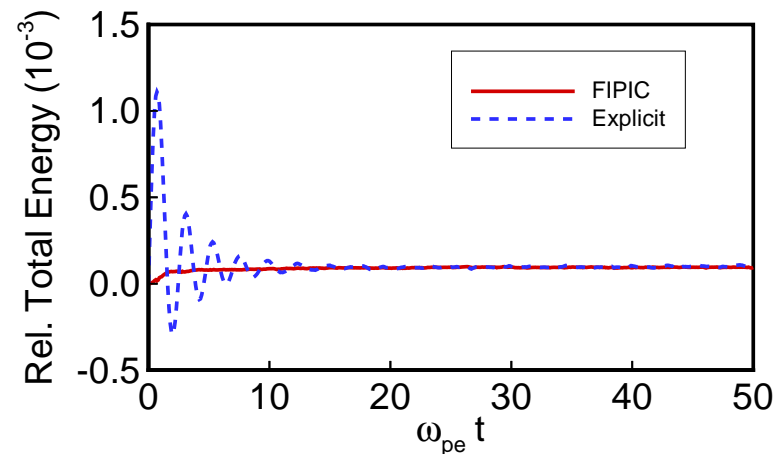
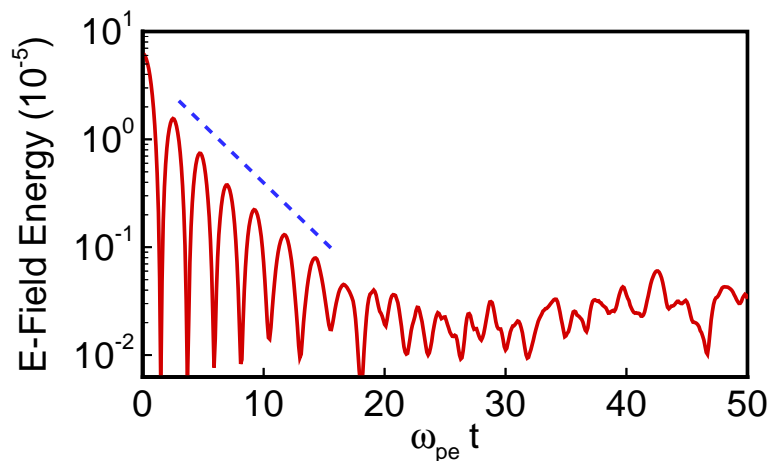
$$\frac{\omega}{\omega_{pe}} = \pm \left[\left(\frac{kv_0}{\omega_{pe}} \right)^2 + \frac{1}{2} \pm \left(2 \left(\frac{kv_0}{\omega_{pe}} \right)^2 + \frac{1}{4} \right)^{1/2} \right]^{1/2}$$



Numerical Test(2): Electron Landau Damping

- **Equilibrium:** uniform density ($n_i = n_e = n_0$), $\vec{E} = 0$, and unmagnetized.
- Immobile ions and **thermal electrons** with Maxwellian distribution.
- 1D domain of 32 grids, 10^5 simulation particles, and $\omega_{pe}\Delta t = 0.1$ **time step**.
- Perturbation of electron density: $\delta n/n_e = \epsilon \cos(k_0\xi)$ with $k_0 = 2\pi$ and $\epsilon = 5 \times 10^{-2}$.
- Linear damping rate $\gamma_{\text{theoretical}} = -0.153$, $\gamma_{\text{simulation}} = -0.146$.

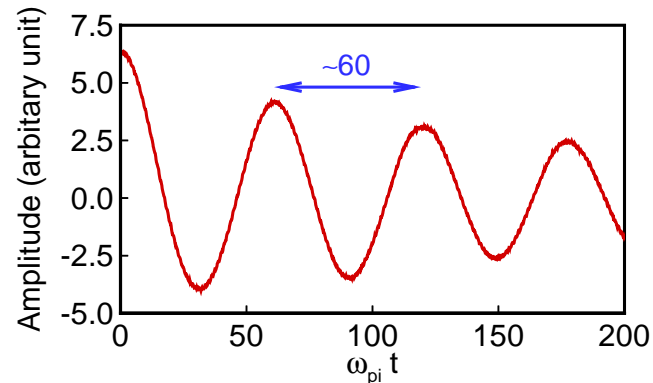
$$\frac{\omega}{\omega_{pe}} \approx 1 + \frac{3}{2}k_n^2\lambda_{De}^2\frac{\omega_{pe}^2}{\omega^2} - i\sqrt{\frac{\pi}{8}}\frac{1}{(k_n\lambda_{De})^3}\exp\left[-\frac{1}{2(k_n\lambda_{De})^2} - \frac{3}{2}\right]$$



Numerical Test(3): Ion Acoustic Wave

- **Equilibrium**: uniform density ($n_i = n_e = n_0$), $\vec{E} = 0$, and unmagnetized.
- **Thermal ions and electrons** with temperatures $T_e/T_i = 100$ and $k\lambda_{De} = 0.1$.
- 1D domain of 64 grids, 10^5 simulation particles, and $\omega_{pi}\Delta t = 0.1$ time step.
- Perturbation of ion and electron densities: $\delta n/n_0 = \epsilon \cos(k_0\xi)$ with $k_0 = 2\pi$ and $\epsilon = 0.1$.
- Frequency of IAW $\omega_{ia}|_{\text{theoretical}} = 9.95 \times 10^{-2}\omega_{pi}$, $\omega_{ia}|_{\text{simulation}} = 1.05 \times 10^{-1}\omega_{pi}$.

$$\omega_{ia} = \frac{kC_s}{\sqrt{1 + k^2\lambda_{De}^2}} = \frac{k\lambda_{De}}{\sqrt{1 + k^2\lambda_{De}^2}}\omega_{pi}$$



(FFT mode 1 ion density history)

Efficiency of Preconditioner

The preconditioner is applied to the Krylov method (GMRES), and its efficiency is demonstrated.

$$P = \nabla_{\vec{\xi}} \cdot \left[\left(1 + (\theta \Delta t)^2 \sum_{\sigma} \frac{q_{\sigma}}{m_{\sigma}} \rho_{\sigma} \right) \nabla_{\vec{\xi}} \right].$$

	preconditioning # of iterations (nonlinear/linear)	no preconditioning # of iterations (nonlinear/linear)
Two Stream	2/4	6/42
Landau Damping	2/4	6/46
Ion Acoustic Wave	3/6	6/60

Grid and Time Step Convergence

- Grid convergence study with $\Delta t = 10\Delta t_{\text{explicit}}$ and 40 time steps for the Ion Acoustic Wave simulation with a mass ratio $m_e/m_i = 1/100$.

Grid	Newton/ Δt	GMRES/ Δt	CPU (s)	$\widehat{\text{CPU}}$
32	4	8	15.4	1.9
64	5	9	31.6	3.5
128	5	10	75.1	7.5
256	6	11	183.4	16.7

($\widehat{\text{CPU}}$ is the CPU time normalized to GMRES/ Δt)

- Time step convergence study with 128 grids for the Ion Acoustic Wave simulation with a mass ratio $m_e/m_i = 1/100$.

Δt	Newton/ Δt	GMRES/ Δt	CPU (s)	$\text{CPU}_{\text{explicit}}/\text{CPU}$	$\Delta t/\Delta t_{\text{explicit}}$
0.5	4	6	110.1	1.3	5
1	5	10	75.1	1.8	10
2	6	14	54.8	2.5	20
3	7	23	63.0	2.2	30

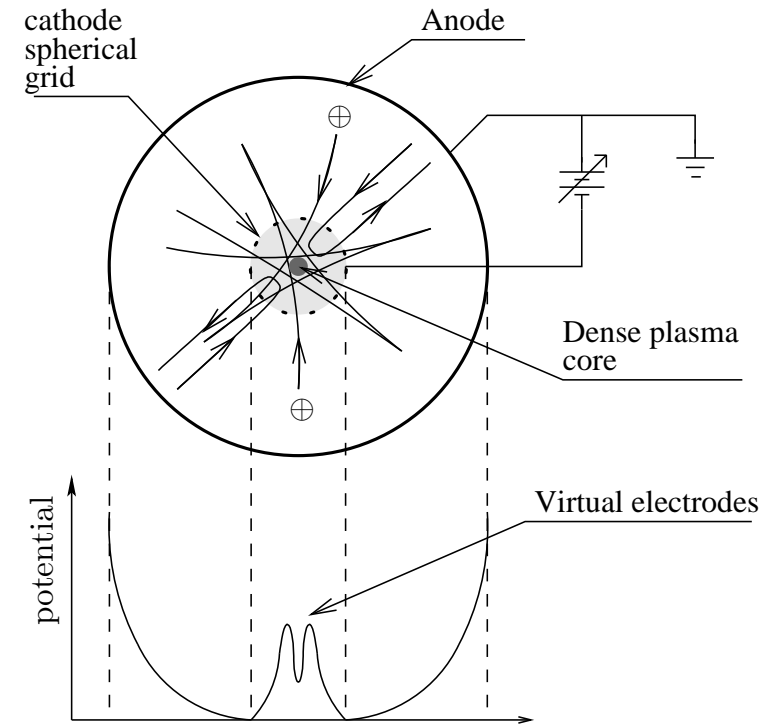
Stability Study on Spherical Inertial Electrostatic Confinement

Inertial Electrostatic Confinement

- **1930-1950**: Inventions regarding electron focusing in cylindrical and spherical vacuum tubes.
- **1950-1960**: Consideration of **concentric spherical grids for production of nuclear fusion reactions** by
 - ▷ Laverentev, Kharkov
 - ▷ Farnsworth, ITT
 - ▷ Elmore, Tuck, and Watson, Los Alamos
- **1960-1980**: Further study of electrostatic plasma confinement at ITT, Kharkov, Illinois, Wisconsin and Penn State.
 - ▷ significantly developed experimentally by Hirsh.
- **1980-2000**: Further study the theoretical issues.
 - ▷ Study the concepts combined with **magnetic confinement** (PollywellTM, PFX-I).
 - ▷ Study the new applications such as **neutron generator**.
 - ▷ Further study the theoretical issues such as **virtual potential well and instability**.

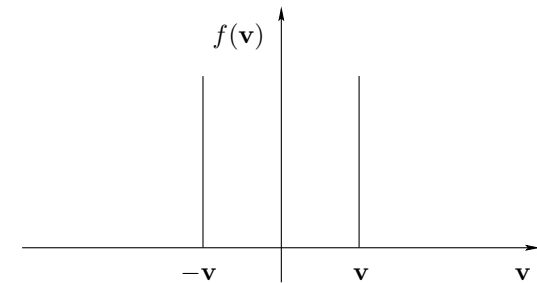
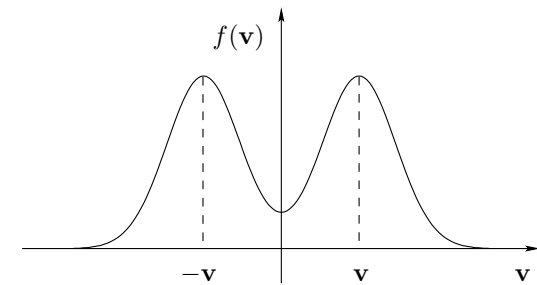
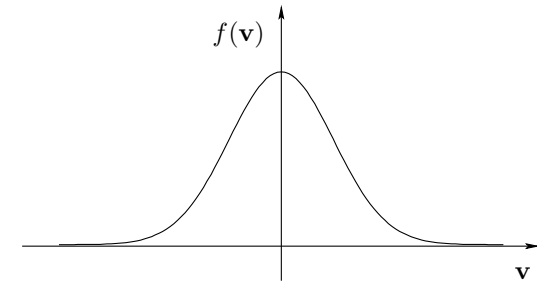
Ion-injected IEC (Background)

- High-voltage is applied between spherical transparent grid (cathode) and spherical vacuum chamber (anode).
- Ions accelerate towards the cathode grid, focus in the center, causing a central virtual anode with high ion density.
- Electrons focus in the center of the virtual anode creating a virtual cathode.
- Ions near the center fuse with each other.



Ion-injected IEC (Properties)

- Highly **non-neutral** (space charge effects).
- Collisionless.
- **Non-thermal equilibrium**.
 - ▷ between a Maxwellian velocity distribution and a two beam velocity distribution (Counter-streaming shifted Maxwellian).
- Need the analysis of **two-stream-like instability** on the base of the kinetic model.



Motivation/goal

- **Two-stream-like instability is the most probable instability of SIEC system.** Particles in SIEC have drift velocities and are spherically converged/diverged.
- Analyses on two-stream instabilities of spherically converging or diverging charged particle beams are **poorly-established**.
- For IEC system, it is increasingly important to develop understanding of instabilities using a **kinetic model based on the nonlinear Vlasov-Poisson equations**.
 - ▷ Space charge effects and collective instabilities (two-stream).
 - ▷ Mode structures, growth rates, and thresholds.
 - ▷ Damping mechanism and wave-particle interaction.
- **GOAL:** to clarify detailed characteristics of **beam instabilities excited in a spherical inertial electrostatic confinement system**.
 - ▷ A kinetic model based on Vlasov-Poisson equations.
 - ▷ Two-stream instability of spherically converging counter-streaming particle beams.
 - ▷ Stability limits for various operation parameters.
 - ▷ δf particle simulation method.

Normal mode analysis in spherical geometry

- Applying a **local theory** (for uniform system) is “**straightforward**”:
JUST DO FOURIER/LAPLACE TRANSFORM → DISPERSION RELATION
- Applying a **nonlocal theory** (for nonuniform system) is “**HARD**” (because Fourier transform cannot be applied): **need a new approach**.
- Consider the following equilibrium system:

$$\nabla \cdot (nv) = 0 \longrightarrow r^2 nv = \text{const},$$

$$n_{i0,\pm}(r) = \frac{\hat{n}_0 r_c^2}{2 r^2}, \quad v_{i0,\pm} = \pm v_0, \quad n_{e0}(r) = 2n_{i0}(r), \quad v_{e0} = 0, \quad \phi_0(r) = \text{const}.$$

- Introduce a **perturbation** in terms of **0th spherical Bessel** (**Gegenbauer’s integral representation**):

$$\delta\phi(r, t) \equiv \sum_l C_l j_0(k_l r) e^{-i\Omega_l t} = \sum_l \frac{C_l}{2} \int_{-1}^1 d\eta e^{i(k_l r \eta - \Omega_l t)}.$$

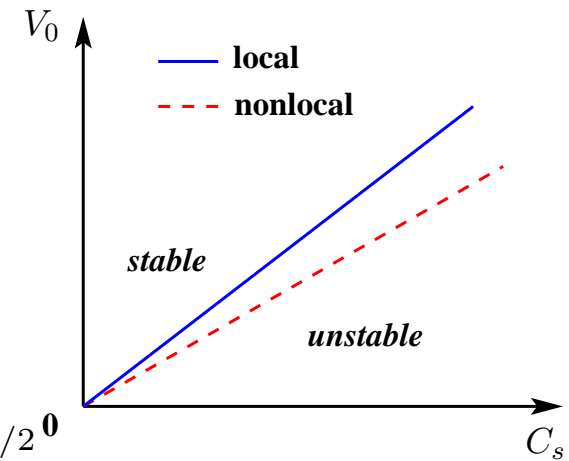
Stability boundary in spherical IEC

- Cold ion beams and hot electron background

$$\frac{v_0}{C_s} < \frac{1}{\sqrt{1 + k^2 \lambda_{De}^2}} \quad (\text{local theory}),$$

$$\frac{v_0}{C_s} < \frac{1}{\sqrt{1 + \kappa (k \lambda_{De,rc})^2}} \quad (\text{nonlocal theory}).$$

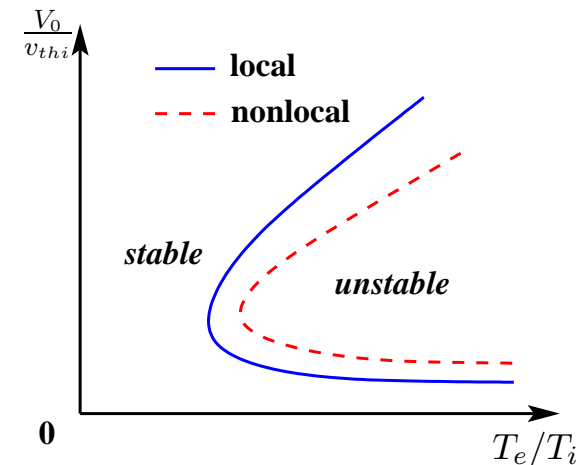
where $\kappa < 1$, $C_s = \sqrt{T_e/m_i}$, and $\lambda_{De,rc} = (T_e/4\pi\hat{n}_0e^2)^{1/2}$.



- Hot ion beams and hot electron background

$$\frac{T_e}{2T_i} \text{Re}Z' \left(\frac{V_0}{2v_{thi}} \right) > 1 \quad (\text{local theory}),$$

not applicable (nonlocal theory).



δf Particle-in-Cell method

- The governing equations which we solve in the electrostatic δf -PIC model consists of the particle weight equations, the trajectory equations, and Poisson's equation for the electric field.

$$\frac{d\omega_{\sigma i}}{dt} = - (1 - \omega_{\sigma i}) \frac{q_{\sigma}}{m_{\sigma}} \delta \mathbf{E} \cdot \frac{1}{f_{\sigma 0}} \frac{\partial f_{\sigma 0}}{\partial \mathbf{v}}, \quad (8a)$$

$$\frac{d\mathbf{x}_{\sigma i}}{dt} = \mathbf{v}_{\sigma i}, \quad (8b)$$

$$\frac{d\mathbf{v}_{\sigma i}}{dt} = \frac{q_{\sigma}}{m_{\sigma}} \mathbf{E} (\mathbf{x}_{\sigma i} (t)), \quad (8c)$$

$$\nabla^2 \delta \phi = -4\pi \sum_{\sigma} q_{\sigma} \sum_{i=1}^{N_{\sigma}} w_{\sigma i} S (\mathbf{x} - \mathbf{x}_{\sigma i}), \quad (8d)$$

where $\omega_{\sigma} \equiv \delta f_{\sigma} / f_{\sigma}$ is the the weight function and $S (\mathbf{x} - \mathbf{x}_{\sigma i})$ is the shape function.

Equilibrium of SIEC

- by setting $\partial/\partial t = 0$ and looking for **stationary solutions** $f_{i0}(\mathbf{x}, \mathbf{v})$ and $\phi_0(\mathbf{x})$ that satisfy the equations

$$\left\{ \mathbf{v} \cdot \frac{\partial}{\partial \mathbf{x}} + \frac{q_\sigma}{m_\sigma} \nabla \phi \cdot \frac{\partial}{\partial \mathbf{v}} \right\} f_{\sigma 0}(\mathbf{x}, \mathbf{v}) = 0, \quad \nabla^2 \phi = -4\pi \sum_\sigma q_\sigma \int d\mathbf{v} f_{\sigma 0}(\mathbf{x}, \mathbf{v}).$$

- **Equilibrium distributions** f_{i0} and f_{e0} are assumed to be

$$f_{i0}(r, v_r, v_\perp) = \hat{f}_{i0} \left[\exp\left(-\frac{m_i(\bar{v}_r - v_b)^2}{2T_{\parallel}}\right) + \exp\left(-\frac{m_i(\bar{v}_r + v_b)^2}{2T_{\parallel}}\right) \right] \exp\left(-\frac{m_i \bar{v}_\perp^2}{2T_\perp}\right),$$

$$f_{e0}(r, v_r, v_\perp) = \hat{f}_{e0} \exp\left(-\frac{m_e(v_r^2 + v_\perp^2) - 2e\phi}{2T_e}\right),$$

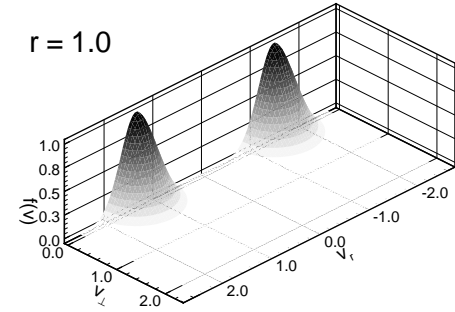
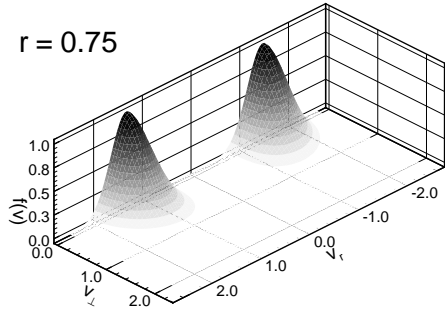
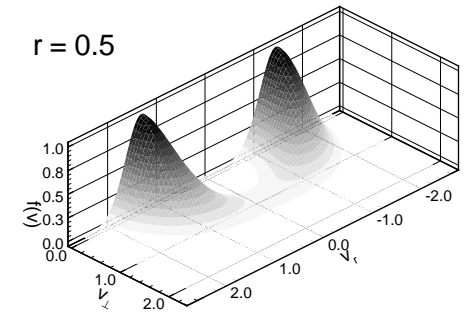
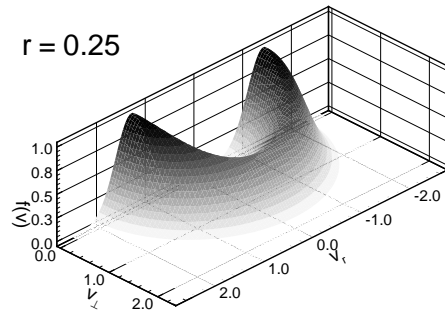
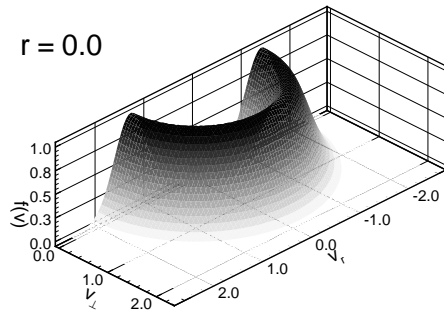
where $\bar{v}_r^2 \equiv v_r^2 + \left(1 - \frac{r^2}{r_c^2}\right) v_\perp^2 + \frac{2q}{m} \phi = \frac{2}{m} (\mathcal{E} - L/2mr_c^2)$ and $\bar{v}_\perp^2 \equiv \frac{r^2}{r_c^2} v_\perp^2$.

- **Equilibrium** ϕ_0 can be determined self-consistently by the Poisson equation

$$\frac{1}{r^2} \frac{\partial}{\partial r} r^2 \frac{\partial}{\partial r} \phi_0(r) = -4\pi e (n_i(r) - n_e(r)),$$

where $n_i(r) = \int d\mathbf{v} f_{i0}(r, \mathbf{v})$ and $n_e(r) = \int d\mathbf{v} f_{e0}(r, \mathbf{v})$.

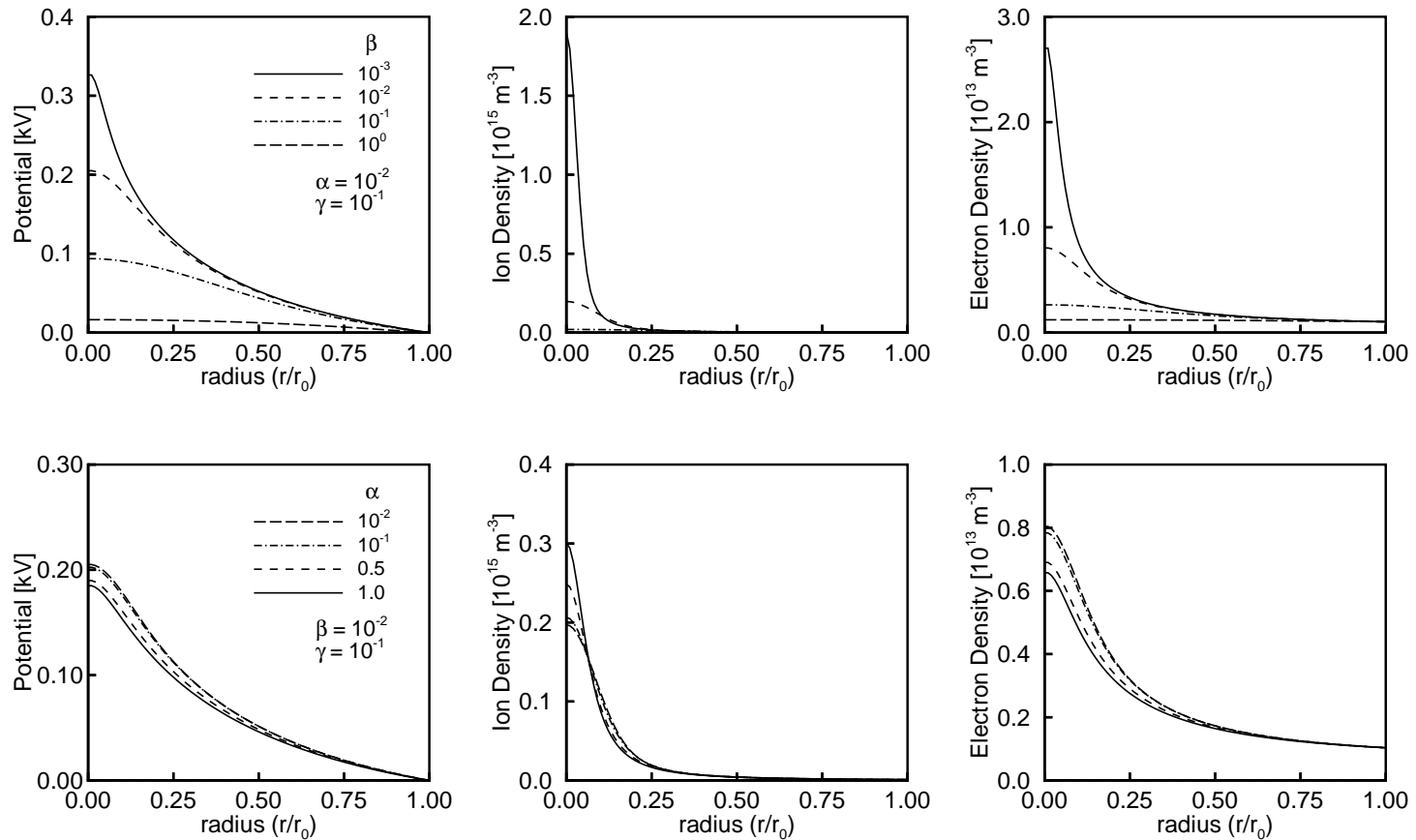
Properties of ion distribution function



- **Drifted Maxwellian** at cathode grid.
- As approaching to centre, **deviated from the drifted Maxwellian** (v_{\perp} increases).

Equilibrium profiles

- Newton-Krylov nonlinear solver and Monte-Carlo method (VEGAS algorithm).

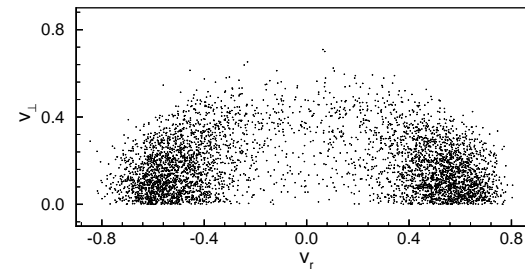
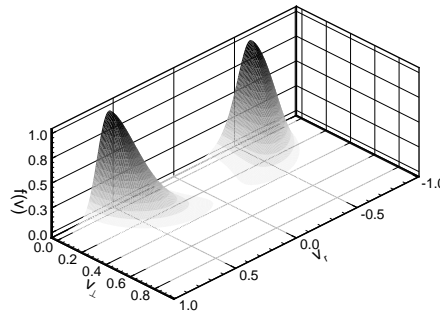


$$(\alpha \equiv |T_{\parallel}/e\phi_c|, \beta \equiv T_{\perp}/|e\phi_c|, \text{ and } \zeta \equiv T_e/|e\phi_c|)$$

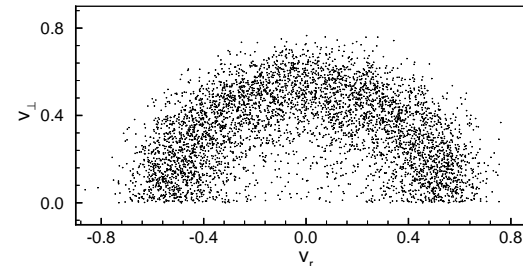
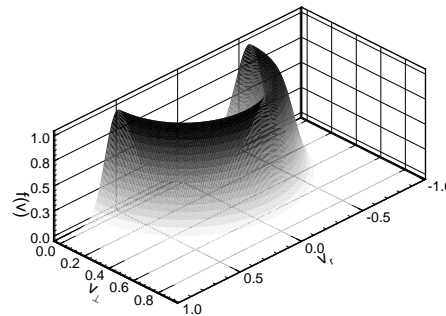
Random variate generation

- **Quality of random variate is very important** because initial particle loading may affect the later behaviour of the system.
- Ion distribution function f_{i0} is **a multivariate function**, i.e., r , v_r , and v_{\perp} .
- For random multivariate generation, **multidimensional kernel density estimate method** is applied.

$r = 0.5$

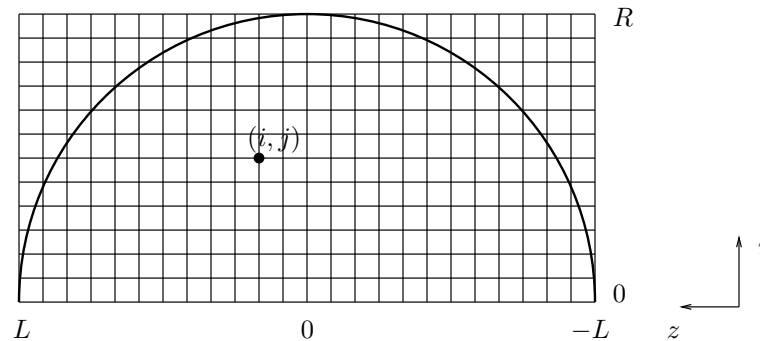


$r = 0$



Computational issues

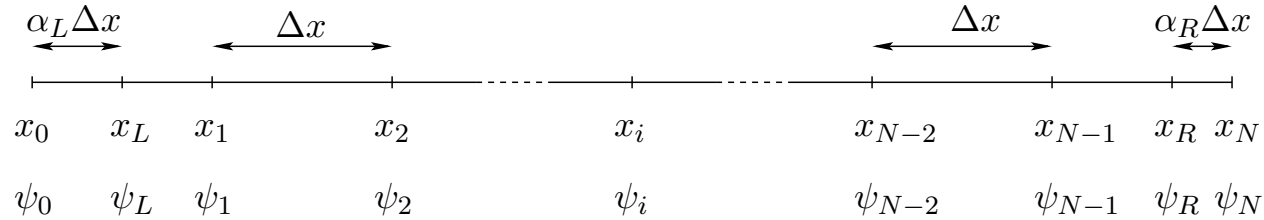
- Geometric effect near at the spherical center may generate the unwanted noise if spherical coordinates system is applied. grid volume ratio: $V_N/V_0 = 3N^2 + 3N + 1$.
- Remedies: (1) increase the number of simulation particles, (2) use non-uniform grid, or (3) **apply cylindrical coordinates system**.
- Poisson solver
 - ▷ **Embedded Boundary Method (EBM)**



Two-dimensional computational domain in cylindrical geometry. The system boundary is depicted inside the rectangular domain with uniform grid cells and represents the sphere.

- ▷ Even for cylindrical system, grid volume ratio is $V_N/V_0 = 2N + 1$. **Non-uniform grid is used**.
- **Transform variables (between spherical and cylindrical)**: $(r, \theta, \varphi) \Leftrightarrow (\rho, \varphi, z), (v_r, v_\theta, v_\varphi) \Leftrightarrow (v_\rho, v_\varphi, v_z)$

Embedded boundary method



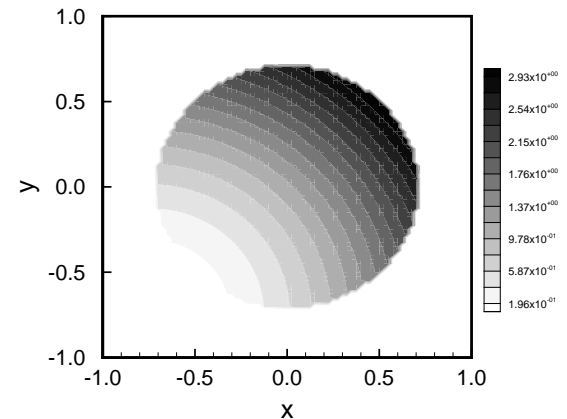
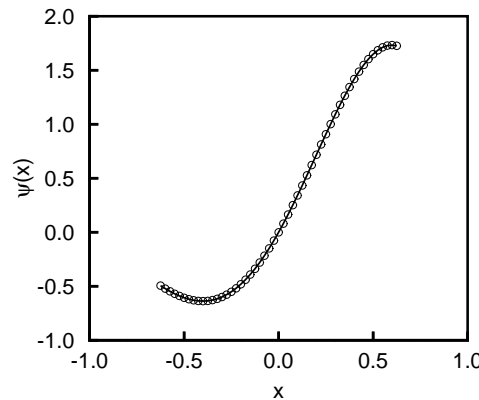
$$\frac{1}{\Delta x} \left(\frac{\psi_{i+1} - \psi_i}{\Delta x} - \frac{\psi_i - \psi_{i-1}}{\Delta x} \right) = \rho_i,$$

$$\frac{1}{\Delta x} \left(\frac{\psi_2 - \psi_1}{\Delta x} - \frac{\psi_1 - \psi_L}{(1 - \alpha_L) \Delta x} \right) = \rho_1, \quad \Rightarrow \quad \begin{pmatrix} A^- & 0 & 0 \\ 0 & A & 0 \\ 0 & 0 & A^+ \end{pmatrix} \begin{pmatrix} \psi^- \\ \psi \\ \psi^+ \end{pmatrix} = \begin{pmatrix} \rho^- \\ \rho \\ \rho^+ \end{pmatrix}$$

$$\frac{1}{\Delta x} \left(\frac{\psi_R - \psi_{N-1}}{(1 - \alpha_R) \Delta x} - \frac{\psi_{N-1} - \psi_{N-2}}{\Delta x} \right) = \rho_{N-1}.$$

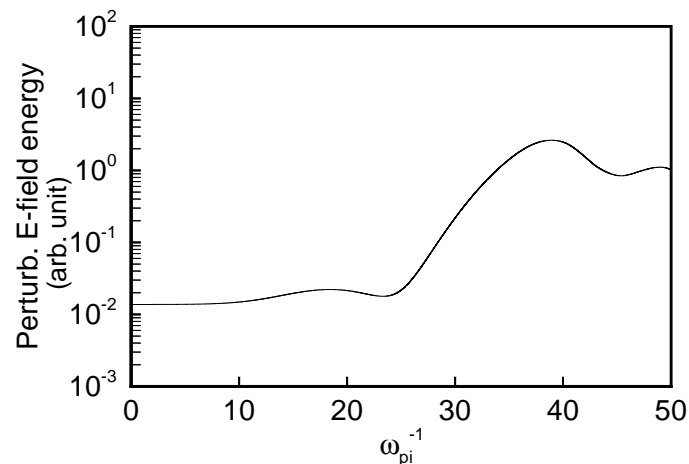
□ $\psi(x) = x^2 \sin(\pi x)$ on $-0.626 \leq x \leq 0.626$ with Dirichlet boundary condition

□ $\psi(x, y) = x^2 + y^2$ on a circular domain with radius $r = 0.713$ with Dirichlet boundary condition



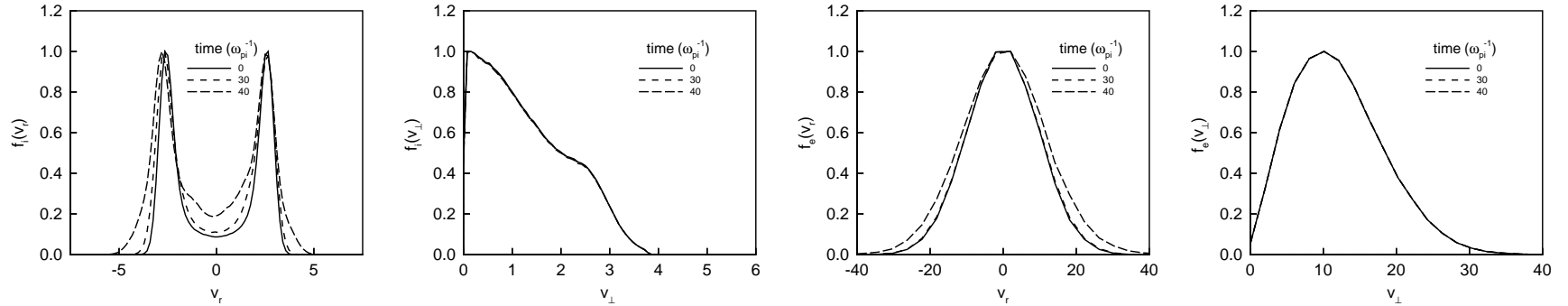
δf simulation:

- **Equilibrium:** spherically symmetric solution ($n_i(r)$, $n_e(r)$, and $\phi(r)$) from self-consistent Poisson equation, and unmagnetized.
- 2D cylindrical domain of 32×64 grids, 10^5 simulation particles, $\omega_{pi}\Delta t = 10^{-3}$ **time step**, and **mass ratio** $m_i/m_e = 100$.
- Initial perturbation of weight: $\delta f/f_0 = \epsilon \sin(k\xi) \sin(\kappa\theta)$, $\epsilon = 10^{-3}$.
- Distribution function parameters: $\alpha = 10^{-2}$, $\beta = 10^{-1}$, $\zeta = 10^0$, and $v_b/\sqrt{2|e\phi_c|/m} = 0.5$. $\Rightarrow v_b/C_s \approx 0.7$.
- Growth rate $\gamma/\omega_{pi,rc} = 2.5 \times 10^{-1}$ for symmetric perturbation.

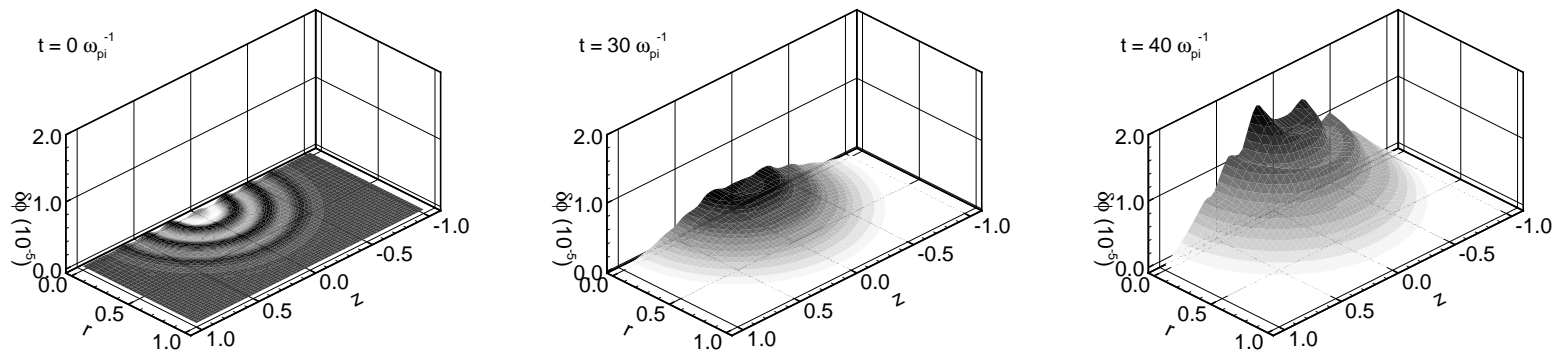


δf simulation: evolution of distribution function

□ Ion and electron distribution functions

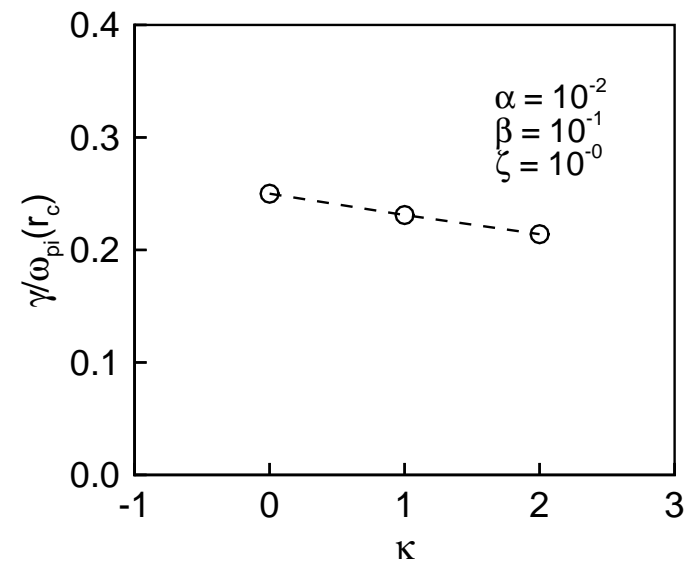
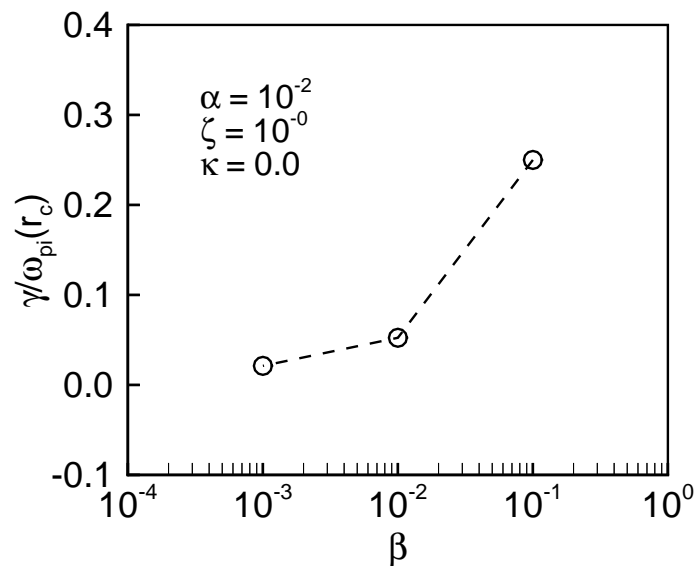


□ Perturbed electrostatic potential $\delta\phi$



δf simulation: growth-rate of two-stream instability

- Growth-rate is obtained for various parameters such as α , β , κ .
 - ▷ $\phi_c = -1.0kV$, $\alpha = T_{\parallel}/|e\phi_c|$, $\beta = T_{\perp}/|e\phi_c|$, and $\kappa = 0 \sim 2$ (angular perturbation).
- Given parameters, the growth rate is **decreased** for **small angular momentum spread**.
- **Symmetric perturbation** gives **high** growth rate.



Summary and conclusion

- A **fully implicit particle-in-cell scheme** has been developed and implemented using a **Jacobian-free Newton-Krylov technique**.
 - ▷ An **efficient preconditioner** is derived from the nonlinear Poisson equation and particle description relations.
 - ▷ The simulation experience presented here demonstrates the **energy conservation property** of the systems and the **efficacy** of nonlinear solver. This technique facilitates simulations of kinetic ion and electron plasma with **multiple time scale**.
- Nonlocal theory in spherical IEC has been developed and applied for seeking **stability boundary** for cold ion beams.
 - ▷ gives complete dispersion relation.
 - ▷ is **applicable** for spherically converging beams.
- **Perturbative (δf) Particle-in-Cell** method has been developed for spherical IEC.
 - ▷ **Combined with EBM**: reduced geometric constraint.
 - ▷ Multivariate random generation with **KDE**.
 - ▷ **Obtained growth rates** for various distribution function parameters and angular perturbations.